13<sup>th</sup> U. S. National Combustion Meeting Organized by the Central States Section of the Combustion Institute March 19–22, 2023 College Station, Texas

# Radiation effects in hydrofluorocarbon/air flames: analysis and development of a spherical flame radiation model

Justin Tavares<sup>1</sup>, Vyaas Gururajan<sup>2</sup>, Jagannath Jayachandran<sup>1\*</sup>

<sup>1</sup>Aerospace Engineering, Worcester Polytechnic Institute, 100 Institute Rd, Worcester, MA 01609, USA

<sup>2</sup>Argonne National Laboratory, 9700 S. Cass Ave., Lemont, IL 60439, USA \*Corresponding Author Email: <u>jjayachandran@wpi.edu</u>

Abstract: Hydrofluorocarbons (HFC), which are mildly flammable and pose potential fire risks, have received greater attention as a viable low global warming potential alternative to traditional refrigerant and fire-suppressant compounds. Therefore, there is a demand to accurately quantify their flammability and reactivity to establish proper safety metrics. This study investigates the effects of radiation heat loss on slowly-propagating HFC/air laminar flames. Simulations of spherically expanding flames (SEF) revealed that the radiation-induced flow needs to be considered when interpreting data from experiments. To this end, a new spherical-flame radiation model was developed to circumvent the effects of radiation-induced inward flow in constant-pressure (CON-P) SEF experimental measurements, accounting for radiation heat loss using the optically thin limit model. The developed spherical-flame radiation model was validated against results from transient SEF simulations.

Keywords: Hydrofluorocarbons, Laminar flame speed, Radiation heat loss, Radiation-induced inward flow

#### 1. Introduction

In the last decade, several major international conferences, such as the Twenty-Eighth Meeting of the Parties to the Montreal Protocol, have promoted the adoption of refrigerants with both lower ozone-depletion potential (ODP) and lower global warming potential (GWP) [1]. A group of hydrofluorocarbon (HFC) compounds have been identified with viable ODP and GWP characteristics [2]. However, this particular group of HFCs are mildly flammable, obeying the general inverse relationship between flammability and GWP [2]. As these mildly flammable HFCs pose potential fire risks, the flammability and reactivity of these compounds need to be quantified in order to establish proper safety metrics [3]. The relative reactivity of flammable HFCs is related to the fluorine-to-hydrogen (F/H) ratio, where a higher F/H ratio corresponds to lower HFC reactivity. Thus, ideal low-GWP candidate HFC refrigerants have been shown to possess relatively low F/H ratios [2,6]. The flammability characteristics of these candidate HFCs have been assessed through the laminar flame speed  $S_u^0$ , a fundamental combustion parameter often used for kinetic

model validation and turbulent combustion scaling [3]. Therefore,  $S_u^0$  must be accurately derived to properly quantify the flammability of HFC/air mixtures.

Spherically expanding flames (SEF) have been widely used to determine  $S_u^0$  using the constant pressure method (CON-P). This configuration uses small amounts of reactants and allows for  $S_u^0$  measurements for a wide range of pressures (e.g., [4,5]). In addition, this configuration effectively contains potentially hazardous burned gas products of HFC mixtures, such as HF, until they can be safely evacuated from the chamber [7,8]. However, derived  $S_u^0$  measurements using the CON-P SEF method for HFC/air flames are often accompanied by large errors and uncertainties caused by the effects of radiation heat loss and buoyancy-induced flow, which have been shown to significantly affect HFC/air flames due to their characteristically low propagation speeds [5,8,9]. The flame shape of slowly-propagating spherical flames is deformed due to gravitational forces; however, this effect can be mitigated by performing experiments under free fall, such as those in a drop tower [10,11,12].

Effects of radiation heat loss have been quantified in flames using several different models, such as the Optically-Thin Limit (OTL) model, which provides an analytical formulation for emission-dominated radiative heat loss flux,  $q_{rad}$  (e.g., [13]). Radiation reabsorption is ignored in the OTL model, but this effect may need to be considered in future work for weak HFC/air flames with relatively large optical thickness [14]. Linteris et al. has considered radiation reabsorption in spherical HFC/air flames, but limited their analysis to solely CO<sub>2</sub> reabsorption, as temperaturedependent absorption efficiencies for HFC refrigerants and their major burned gas products are currently unavailable [14]. Reductions in flame propagation speed due to radiation heat loss have been extensively studied for near-limit hydrocarbon/air flames [15,16,17,18,19]: (1) radiation heat loss and conduction from the flame zone reduces the maximum flame temperature and the overall chemical reactivity, consequently lowering flame propagation speed and (2) radiation-induced inward flow, generated by the burned gas contraction from radiative cooling, reduces flame propagation speeds in the lab frame of reference. Flame speed reductions due to flame zone losses exist in all flames (e.g. planar, spherical, etc.), while reductions due to induced inward flow are primarily associated with spherical flames. Large flame zone losses are characteristic of weakly propagating flames, where the time scale of radiative heat loss from the flame is comparable to that of flame propagation [16]. For instance, large flame zone losses are often observed in flames whose unburned gas mixture composition approaches the lower flammability limit (LFL) in hydrocarbon/air flames [16]. Furthermore, for slowly propagating flames (weak, near-limit hydrocarbon/air flames and strongly burning high pressure flames), the effect of radiation-induced inward flow has been shown to cause large errors in  $S_u^0$  derived using the SEF experiment [16]. Therefore, there is a need to study and quantify radiation effects in weakly-propagating HFC/air flames.

Radiation induced inward flow can be accounted for while interpreting SEF data through analytical/numerical models. Simultaneous measurement of flow velocity and expansion rate can enable accurate determination of  $S_u^0$ . However, such measurements are especially challenging in free-fall experiments [18]. Estimates for flame speed reductions due to flame zone losses in radiative flames have been performed in previous studies [19,20]. For correcting the inward flow effect in spherical flames, Santner et al. derived an analytical model to quantify the radiation-induced inward flow velocity  $u_b$  in hydrocarbon/air mixtures for the CON-P SEF configuration [19]. This model evaluates burned gas parameters, including the Planck mean absorption coefficient, at the adiabatic flame temperature and equilibrium mole fractions. In addition,

Santner's model is derived from a simplified energy conservation equation, assuming that conductive and convective heat transfer have negligible contributions relative to radiation heat loss. The inward flow velocity  $u_b$  is then subtracted from the flame propagation speed  $dR_f/dt$ , derived from flame radius  $(R_f)$  vs. time (t) data, to circumvent the inward flow effect in radiative, spherical flames. Santner et al. showed that using this model to account for the radiation-induced flow effect while deriving the burned flame speed improved the accuracy of  $S_u^0$  for hydrocarbon/air flames at elevated pressures [19]. Hesse et al. applied Santner's model to HFC/air flames at elevated initial temperatures and pressures for stoichiometric  $CH_2F_2$  (R-32) mixtures, showing decent agreement with Santner's analytical model for flame radii within the typical experimental range [8]. However, it is not clear whether the assumptions utilized in Santner's model are valid for weaker, less reactive flames (e.g., non-stoichiometric HFC/air flames at ambient conditions) [20]. Therefore, numerical models with fewer assumptions than Santner's model may be necessary to properly quantify  $u_b$  for HFC/air flames at various conditions of interest.

Numerical simulations, utilizing detailed chemical kinetic models, have been used to compute the spatial profile for gas velocity as a function of time, from which  $u_b$  has been derived as the minimum of gas velocity profile as often done in the literature [9,16,17,21]. However, reaction rates involving fluorine chemistry are often estimated within detailed chemical kinetic models, potentially introducing large uncertainties and inaccuracies; therefore, such models are not suitable for interpreting experimental data. Xiouris et al. developed a Hybrid ThermoDynamic-Radiation (HTDR) model, which interprets experimental data by quantifying the effect of radiative cooling on  $S_u^0$  for the constant volume (CON-V) SEF configuration [22]. The HTDR model accounts for finite-rate radiation heat loss using a time scale derived from experimental measurements, thus avoiding potentially unreliable chemical kinetic data. However, a similar model does not exist for interpreting experimental data using the CON-P SEF method.

To properly quantify the flammability of HFC/air mixtures, the laminar flame speed  $\Box_{\Box}^{0}$  must be accurately derived accounting for the effects of radiation. To this end, the major objective of this study is to develop and validate a numerical radiation model which can properly interpret CON-P SEF experimental data, circumventing the effects of radiation-induced inward flow.

#### 2. Methods

## 2.1. Spherical HFC/air flame simulation

Transient, 1-D, SEF simulations at constant pressure were performed using the reacting flow code SLTORC, a modified version of the TORC code [23], which solves the governing reacting flow conservation equations in Lagrangian coordinates [24], utilizing operator splitting to overcome gridding and initialization difficulties present in the fully coupled Differential Algebraic Equation (DAE) code TORC. Chemical models for R-32 and R-1234yf combustion were obtained from Babushok et al. [3,25,26]. The R-1234yf chemical model was reduced utilizing the Directed Relations Graph method, thus minimizing computational costs for R-1234yf/air numerical simulations [27]. Radiation was accounted for by utilizing the OTL model. The source code was

modified to include Planck mean absorption coefficients (radiation coefficients) for the fluorinated compounds HF and CF<sub>2</sub>O, obtained from Fuss & Hamins [28]. SLTORC flame simulations, specifically constant-pressure spherical flames, are initialized by a kernel of hot burned gas with a hyperbolic tangent temperature profile which transitions from burned to unburned conditions. The ignition energy is controlled through parameters specifying the initial kernel radius and temperature such that the effect of ignition energy on flame propagation was minimized. The time-evolution of the flame radius is determined using a user-specified isotherm, which was chosen so that radiative cooling in the burned gas would not interfere with flame radius tracking. Convergence tests were conducted to determine proper values for parameters controlling grid refinement and time step size to allow for grid-independent solutions. SLTORC results were post-processed to determine the flame speed evolution with decreasing flame stretch rate, as well as the radiation-induced inward flow velocity. Flame speeds were then corrected for radiation-induced inward flow effects, allowing the burned flame speed to be properly compared to zero-stretch  $S_b^0$  results from Cantera planar simulations.

# 2.2. Spherical radiation model development

A Spherical RADiation-Induced Flow (SRADIF) model was developed to quantify radiation-induced inward flow effects in spherical HFC/air flames. The SRADIF model was used to estimate  $u_b$  in CON-P SEF experiments, thereby enabling accurate determination of  $S_u^0$ . The model is inspired by the HTDR model for the CON-V SEF method developed by Xiouris et al. [22]. The total gas volume is initially divided into layers of thin spherical shells of equal width. The model uses flame radius  $R_f$  vs. time t experimental data as an input. All thermodynamics calculations are performed using the equilibrium calculation functionalities of Cantera [29]. Each algorithm step corresponds to the combustion of the next unburned gas shell, for which the following sub-steps are performed:

- 1. The combustion of the current gas shell is modeled as an equilibrium process under the constraints of constant pressure (P) and enthalpy (h). Once equilibrated, the gas shell achieves its maximum temperature, at which burned gas species mole fractions correspond to those at the adiabatic flame temperature. Due to constant pressure conditions, the total gas volume increases as the volume of the combusted gas shell increases.
- 2. Dissociation for all previously burned gas shells is modeled with the same equilibrium process as described in Step 1. The new burned gas shell volumes and species mole fractions are computed, and the current flame radius position  $R_{f,1}(t)$  is recorded. This step accounts for the change in equilibrium state due to changes in temperature from radiative cooling.
- 3. The change in temperature per unit time due to radiative cooling is calculated for each burned gas shell, according to the formula below. The radiative heat loss is calculated using the OTL radiation model, in which individual heat loss contributions are calculated for major product and intermediate species (CO<sub>2</sub>, HF, CO, and CF<sub>2</sub>O) using Planck mean absorption coefficients according to Eq. (1): [13]

$$\left. \frac{\partial T}{\partial t} \right)_{rad} = \frac{1}{\rho c_p} \left( 4\sigma P \sum_{i} X_i K_{p,i} (T^4 - T_0^4) \right) \tag{1}$$

- 4. The radiative cooling time  $\Delta t_{rad}$  is found through an iterative approach using linear interpolation between flame radius  $R_f$  vs. time t experimental data. The pre-cooling flame radius  $R_{f,1}(t)$  is recorded for use in Step 5, while the post-cooling flame radius  $R_{f,2}$  is computed by summing the change in shell thicknesses after applying Eq. (1) to all previously burned gas shells.
- 5. The radiation-induced inward flow velocity  $u_b$ , (i.e. the minimum of the  $u_{rad}(r)$  curve) is calculated by dividing the total burned gas contraction by the radiative cooling time according to Eq. (2):

$$u_b = \frac{R_{f,2} - R_{f,1}}{\Delta t_{rad}} \tag{2}$$

This algorithm is repeated for each subsequent shell until either all shells have been burned or simulated burned gas radius exceeds the final radius of the input experimental data. For validation purposes, spherical SLTORC flame simulation time-radius results were used as the "experimental" data for the SRADIF model. This allowed for the  $u_b$  computed from the SRADIF model to be directly compared to that derived from the SLTORC simulation results.

### 2.3. Radiation-induced flow velocity derivation

In quasi-1-D spherical flames, gas velocity u(r,t) is a function of radius and time. At a particular time, the gas velocity varies as a function of radius. For chemically reacting flows at constant pressure in spherical Eulerian coordinates, the observed or "total" gas velocity u(r) can be computed using Eq. (3), derived from the continuity equation: [29]

$$u(r) = -\frac{1}{\rho r^2} \int_0^r \frac{\partial(\rho \bar{r}^2)}{\partial t} \bar{r}^2 d\bar{r}$$
 (3)

Furthermore, the value of  $u_b$  is commonly derived as the minimum of u(r), which occurs in the burned gas in the proximity of the flame zone [9,16,17]. However, there are several ambiguities with the conventional method of estimating  $u_b$  as the minimum of u(r). Firstly, this minimum occurs at an arbitrary location in the burned gas. Secondly, the total gas velocity u(r) may not be the most adequate flow velocity for deriving  $u_b$ , which should only consider the radiation heat loss term. By isolating the radiation heat loss term in the governing energy equation, the radiation losses in the burned gas can be quantified by the radiation-induced gas velocity  $u_{rad}(r)$ . For a constant pressure, spherical flame, this corresponds to radiation-induced changes in density due to cooling in the burned gas. To validate the SRADIF model, a proper formula for  $u_{rad}(r)$  must be derived. Santner et al. and Yu et al. both derived equations for  $u_b$  from a simplified energy equation, in which the convective term was deemed to be negligible compared to thermal conduction, mass diffusion, and chemical heat release [17,19]. The continuity equation and energy conservation equation considering only radiation heat loss, are given in Eq. (4) and Eq. (5), respectively [19]:

$$\frac{\partial \rho}{\partial t} + \frac{1}{r^2} \frac{\partial (\rho u r^2)}{\partial r} = 0 \tag{4}$$

$$\rho c_p \frac{\partial T}{\partial t} = -q_{rad} \tag{5}$$

Substituting the energy conservation equation into the continuity equation, an equation for  $u_{rad}(r)$  was derived according to Eq. (6):

$$u_{rad,no-conv}(r) = -\frac{1}{\rho r^2} \int_0^r \frac{q_{rad}}{c_p T} \bar{r}^2 d\bar{r}$$
 (6)

However, this approach ignores a potentially important coupling between the convective terms of the continuity and energy conservation equations [19]. Therefore, a new equation for  $u_{rad}$  was derived from the governing conservation equations by including the convective term in the energy equation. The conservation of energy equation for radiation heat loss with convective term coupling is given in Eq. (7):

$$\rho c_p \frac{\partial T}{\partial t} + \rho u c_p \frac{\partial T}{\partial r} = -q_{rad} \tag{7}$$

In a similar approach, an equation for  $u_{rad}(r)$ , now including convective term coupling, was derived according to Eq. (8):

$$u_{rad,conv}(r) = -\frac{1}{r^2} \int_0^r \frac{q_{rad}}{\rho c_p T} \bar{r}^2 d\bar{r}$$
 (8)

#### 3. Results and Discussion

#### 3.1. Spherical HFC/air flame simulation

Transient, spherically-symmetric quasi-1-D HFC/air flame simulations were performed for various R-32/air and R-1234yf/air mixtures, accounting for radiation heat loss in the burned gas. The total radiation heat loss  $q_{rad}(r)$  was computed at each time step by summing the heat loss contribution from major radiating species. The variation of  $q_{rad}(r)$  in the burned gas was examined at specified time instances in which the flame had reached quasi-steady propagation (i.e. ignition-related effects had dissipated). As flow velocities are more practical for quantifying the effect of radiation heat loss on flame propagation speed, the inward flow velocity  $u_{rad}(r)$  was derived from  $q_{rad}(r)$  through the two formulations (Eq. 6 and Eq. 8) provided in section 2.3. Sample results for the radial profiles of  $q_{rad}(r)$  and  $u_{rad}(r)$  for an R-32/air flame are shown in Figure 1, in which the derived  $u_{rad}(r)$  profiles are compared to that of  $u_{total}(r)$ . Comparing the two derived  $u_{rad}(r)$  profiles in Figure 1b, the greatest difference occurs in the unburned gas (approx. between 5-7 cm). Here,  $u_{rad,conv}(r)$  (including the energy equation convective term)

shares the same  $\frac{1}{r^2}$  trend as  $u_{total}(r)$ . This trend is to be expected for constant-pressure, spherical flames, for which the thermodynamic state of the unburned gas remains constant and spatially uniform. Further, the convective term of the energy equation cannot be deemed negligible in such derivations, as convective term coupling between the continuity and energy equations is significant in terms of producing expected flow behavior in the unburned gas. Thus,  $u_{rad,conv}(r)$  was chosen as the correct formulation for deriving the radiation-induced inward flow  $u_b$  in spherical flames. Additionally, in Figure 1b, there is an appreciable difference between the minima of  $u_{rad,conv}$  and  $u_{total}$ . Using the minimum of  $u_{total}(r)$ , which is affected by both radiation heat loss and local heat release, as the conventional method for computing  $u_b$  can potentially underpredict  $u_b$  by upwards of 30% compared to using the minimum of  $u_{rad,conv}(r)$ . Therefore, the minimum of  $u_{total}(r)$  is inadequate for accurately estimating  $u_b$  in spherical HFC/air flames.

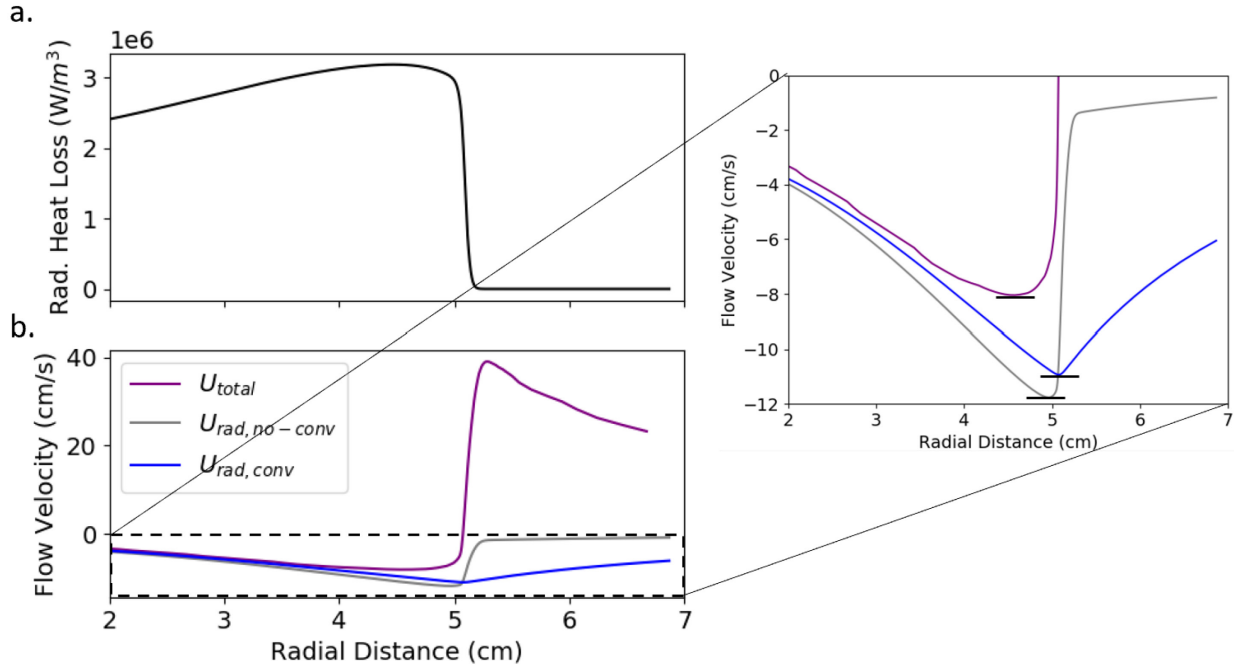


Figure 1: Spherical, quasi-steady, R-32/air flame with initial  $\phi$ =1.2, 1 atm and 300 K: a.) Radiation heat loss vs. radial distance, b.) Gas flow velocity vs. radial distance.

## 3.2. Validation of the spherical radiation model

The Spherical RADiation-Induced Flow (SRADIF) model was tested using spherical, HFC/air flame simulation (SLTORC) results. The radiation-induced flow velocity  $u_{rad}(r)$  was computed using the SRADIF model for times at which the flame reached quasi-steady propagation.

An example of this flow velocity profile is shown in Figure 2, which compares the flow velocity from the SRADIF model to the flow velocity computed using simulation results (i.e.  $u_{rad,conv}(r)$  using Eq. (8)). Figure 2 shows that the SRADIF model accurately predicts the inward flow behavior in the burned gas compared to simulations results. In addition, by comparing the minima of the  $u_{rad}(r)$  curves in Figure 2, the SRADIF model provides an accurate estimate for the magnitude of  $u_b$ . This value for  $u_b$  can then be subtracted from the flame propagation speed  $dR_f/dt$  to give the corrected flame propagation speed, circumventing radiation-induced inward flow effects.

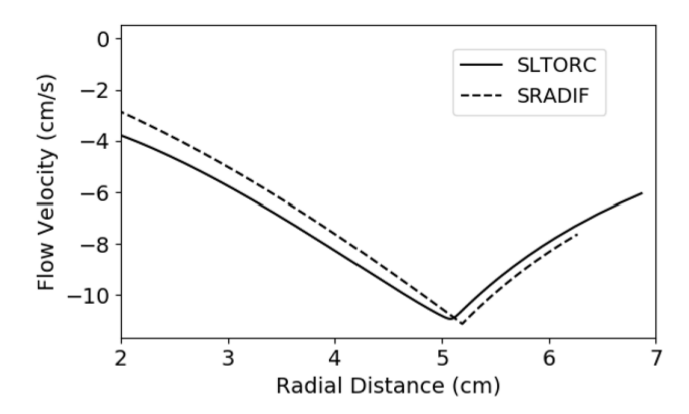


Figure 2: Spherical, quasi-steady, R-32/air flame with initial  $\phi$ =1.2, 1 atm and 300 K: Radiation inward flow profile  $u_{rad}(r)$  vs. radial distance comparing simulation (SLTORC) results to radiation modeling (SRADIF) results.

# 4. Conclusions

Radiation has been shown to significantly affect HFC/air flames due to their characteristically low propagation speeds. Therefore, radiation effects in HFC/air flames must be studied and quantified in order to accurately derive  $S_u^0$  from experimental measurements. A spherical-flame radiation model (SRADIF) was developed to interpret CON-P SEF experimental measurements, circumventing the effects of radiation-induced inward flow. This model was validated against spherical-flame simulations using a newly-derived formulation for radiation-induced gas flow velocity with convective term coupling.

## 5. Acknowledgements

This research was funded by the National Science Foundation (NSF) [CBET-2053239].

#### 6. References

[1] UNEP Ozone Secretariat. in Twenty-Eighth Meeting of the Parties to the Montreal Protocol on Substances that Deplete the Ozone Layer (Kigali, Rwanda, 2016); document UNEP/OzL.Pro.28/CRP/10, United Nations Environment Programme, (2016).

- [2] Takizawa et al., Flammability assessment of CH2=CFCF3: Comparison with fluoroalkenes and fluoroalkanes, *Journal of Hazardous Materials* 172 (2009) 1329–1338.
- [3] V.I. Babushok, D.R. Burgess Jr., D. Kim, M. Hegetschweiler, G.T. Linteris, Modeling of Combustion of Fluorine-Containing Refrigerants, NIST Technical Note 2170 (2021).
- [4] F.N. Egolfopoulos et al., Advances and challenges in laminar flame experiments and implications for combustion chemistry, *Progress in Energy and Combustion Science* 43 (2014) 36-67.
- [5] R.R. Burrell, J.L. Pagliaro, G.T. Linteris, Effects of stretch and thermal radiation on difluoromethane/air burning velocity measurements in constant volume spherically expanding flames, *Proceedings of the Combustion Institute* 37 (2019) 4231-4238.
- [6] R.R. Burrell, G.T. Linteris, D.R. Burgess, M.J. Hegetschweiler, J.A. Manion, V. Babushok, R-152a/air and R-134a/oxygen constant volume spherical flame burning velocity measurements, 11th U. S. National Combustion Meeting, Pasadena, CA, 2019.
- [7] Takizawa et al., Burning velocity measurement of fluorinated compounds by the spherical-vessel method, *Combustion and Flame* 141 (2005) 298-307.
- [8] Hesse et al., Low global-warming-potential refrigerant CH2F2 (R-32): Integration of a radiation heat loss correction method to accurately determine experimental flame speed metrics, *Proc. Combust. Inst.* 38(3) (2021) 4665-4672.
- [9] Hegetschweiler et al., Effects of stretch and radiation on the laminar burning velocity of R-32/air flames, *Science and Technology for the Built Environment* 26(5) (2020) 599-609.
- [10] Choi et al., Characteristics of outwardly propagating spherical flames of R134a(C2H2F4)/CH4/O2/N2 mixtures in a constant volume combustion chamber, *Energy* 95 (2016) 517-527.
- [11] Berger et al., A DNS study of the impact of gravity on spherically expanding laminar premixed flames, *Combustion and Flame* 216 (2020) 412-425.
- [12] Qiao et al., Extinction of premixed methane/air flames in microgravity by diluents: Effects of radiation and Lewis number, *Combustion and Flame* 157(8) (2010) 1446-1455.
- [13] C.K. Law & F.N. Egolfopoulos, A unified chain-thermal theory of fundamental flammability limits, *Symposium (International) on Combustion* 24(1) (1992) 137-144.
- [14] D. R. Burgess Jr. et al., Burning velocities of R-32/O2/N2 mixtures: Experimental measurements and development of a validated detailed chemical kinetic model, *Combustion and Flame* 236 (2022).
- [15] Ju et al., On the extinction limit and flammability limit of non-adiabatic stretched methaneair premixed flames, *Journal of Fluid Mechanics* 342 (1997) 315-334.
- [16] Z. Chen, Effects of radiation and compression on propagating spherical flames of methane/air mixtures near the lean flammability limit, *Combustion and Flame* 157 (2010) 2267-2276.
- [17] Yu et al., Radiation-induced uncertainty in laminar flame speed measured from propagating spherical flames, *Combustion and Flame* 161 (2014) 2815-2824.
- [18] Jayachandran et al., Determination of laminar flame speeds using stagnation and spherically expanding flames: Molecular transport and radiation effects, *Combustion and Flame* 161 (2014) 2305-2316.
- [19] Santner et al., Uncertainties in interpretation of high pressure spherical flame propagation rates due to thermal radiation, *Combustion and Flame* 161 (2014) 147-153.
- [20] Ju et al., Effects of radiative emission and absorption on the propagation and extinction of premixed gas flames, *Proc. Combust. Inst.* 27(2) (1998) 2619-2626.

- [21] Linteris et al., Data reduction considerations for spherical R-32(CH2F2)-air flame experiments, *Combustion and Flame* 237 (2022) 111806.
- [22] Xiouris et al., Burning velocities of R-32/O2/N2 mixtures: experimental measurements and development of a validated detailed chemical kinetic model, *Combustion and Flame* 163 (2016) 270-283.
- [23] V. Gururajan, J. Jayachandran, "SLTORC: An Operator Split One-Dimensional Reacting Flow Code in Lagrangian Coordinates" (unpublished manuscript, August 29 2022), typescript.
- [24] Bradley et al., Burning velocities, Markstein lengths, and flame quenching for spherical methane-air flames: A computational study, *Combustion and Flame* 104(1-2) (1996) 176-198.
- [25] V.I. Babushok, D.R. Burgess Jr, M.J. Hegetschweiler, G.T. Linteris, Flame propagation in the mixtures of O2/N2 oxidizer with fluorinated propene refrigerants (CH2CFCF3, CHFCHCF3, CH2CHCF3), *Combust. Sci. Technol.* 193 (2021) 1949-1972.
- [26] Valeri I. Babushok, Gregory T. Linteris, Kinetic Mechanism of 2,3,3,3-Tetrafluoropropene (HFO-1234yf) *Combustion, Journal Fluor. Chem.* 201 (2017) 15-18.
- [27] P. O. Mestas, P. Clayton, and K. E. Niemeyer. (2019) pyMARS v1.1.0 [software]. Zenodo.
- [28] S.P Fuss, A. Hamins, Determination of Planck mean absorption coefficients for HBr, HCl, and HF, *Journal of Heat Transfer* 124(1) (2002) 26-29.
- [29] D.G. Goodwin, R.L. Speth, H.K. Moffat, B.W. Weber, Cantera: An object-oriented software toolkit for chemical kinetics, thermodynamics, and transport processes. https://www.cantera.org, 2021. Version 2.5.0.